Journal of Marine Systems 188 (2018) 3–16

Contents lists available at ScienceDirect

Journal of Marine Systems

journal homepage: www.elsevier.com/locate/jmarsys

Upwelling indices for comparative ecosystem studies: Variability in the Benguela Upwelling System

T. Lamont [a,b,*], M. García-Reyes [c], S.J. Bograd [d], C.D. van der Lingen [e,f], W.J. Sydeman [c,g]

[a] Oceans & Coasts Research Branch, Department of Environmental Affairs, Private Bag X4390, Cape Town 8000, South Africa
[b] Marine Research Institute and Department of Oceanography, University of Cape Town, Private Bag X3, Rondebosch 7701, South Africa
[c] Farallon Institute, 101 H St. Suite Q, Petaluma, CA 94952, USA
[d] Environmental Research Division, Southwest Fisheries Science Center, NOAA, Monterey, California, USA
[e] Branch: Fisheries Management, Department of Agriculture, Forestry and Fisheries, Private Bag X2, Rogge Baey, 8012, South Africa
[f] Marine Research Institute and Department of Biological Sciences, University of Cape Town, Private Bag X3, Rondebosch 7701, South Africa
[g] Bodega Marine Laboratory, University of California, Davis, P.O. Box 247, Bodega Bay, CA 94923, USA

ARTICLE INFO

Article history:
Received 1 January 2017
Received in revised form 5 May 2017
Accepted 19 May 2017
Available online 24 May 2017

Keywords:
Benguela upwelling system
Ekman transport
Upwelling indices
South Atlantic high pressure system

ABSTRACT

The influence of climate variability on Eastern Boundary Upwelling Ecosystems (EBUEs) is evident through changes in productivity and shifts in species' distributions, yet to date, metrics of upwelling variability appropriate for comparative ecosystem studies have yet to be implemented. Here, we present synoptic-scale upwelling indices to quantify inter-annual to decadal variations in Ekman transport, at temporal and spatial scales relevant to the biota of EBUEs, and apply them to the Benguela Upwelling System (BUS). From 1979 to 2015, interannual, decadal-scale, and unidirectional variability in upwelling was observed, including a significant recent decrease in upwelling in the northern BUS, and a significant increase on the Agulhas Bank. These trends are associated with changes in the number of upwelling days and events in these regions, and correspond to a shift in the meridional positioning of the South Atlantic High pressure system.

1. Introduction

Comparative studies of similar systems facilitate the resolution of effects of natural and anthropogenic climate change on marine ecosystems. The four major Eastern Boundary Upwelling Ecosystems (EBUEs) are uniquely significant to society owing to their contributions to fisheries (Pauly and Christensen, 1995), as well as their hypothesized role in modulating earth's climate (IPCC, 2014). It is thought that anthropogenic climate change is affecting EBUE productivity and the distribution and abundance of fish and other biota via changes in regional upwelling (IPCC, 2014; Sydeman et al., 2014), but metrics of upwelling appropriate for detailed comparative studies among EBUEs, at temporal scales useful for investigating biological patterns and variability, have yet to be implemented.

While the well-known large-scale geostrophic Upwelling Index (UI, Bakun, 1973) has proven useful for understanding the California Upwelling System (CUS) dynamics (e.g. García-Reyes et al., 2013), newer upwelling indices based on the synoptic (event) scale have been derived for the CUS (Iles et al., 2012; García-Reyes et al., 2014), but are lacking for other systems. In the BUS, several authors (Roy et al., 2001; van der Lingen et al., 2016, among others] have demonstrated the importance of event-scale upwelling by illustrating substantial impacts of individual events on phytoplankton and fish abundances and distributions. In this paper, we use synoptic-scale upwelling indices based on reanalysis data to quantify and describe inter-annual to decadal variations in Ekman transport, at temporal and spatial scales relevant to the biota of EBUEs (e.g. Schroeder et al., 2013). This new effort is designed to extend the previous results of Bograd et al. (2009) who focused on the seasonality of upwelling in the CUS, to facilitate comparisons of upwelling-ecosystem dynamics of the world relative to climate change, while still capturing the totality of wind-driven Ekman transport through the year. As a new case study, we focus on the Benguela Upwelling System (BUS), but note that these upwelling indices can be applied to each of the other EBUEs.

Among EBUEs, the BUS is unique in that it is bounded by warm waters at both its northern (Angola-Benguela Front) and southern (Agulhas Current) limits (Shillington et al., 2006). The BUS is separated into the northern and southern subsystems at Lüderitz (27.5°S), where perennial upwelling forms an environmental barrier which is thought to limit the exchange of epipelagic biota between these subsystems (Lett et al., 2007; Hutchings et al., 2009). The primary mode of variability differs between these regions, indicating potential differences in the forcing mechanisms between these two west coast regions of the BUS (Hutchings et al., 2009). For within- and between-upwelling system comparative analyses, we sought to derive regional upwelling indices. In addition, we produced indices for the south coast of South Africa

* Corresponding author.
E-mail address: tarron.lamont@gmail.com (T. Lamont).

http://dx.doi.org/10.1016/j.jmarsys.2017.05.007
0924-7963/

(Agulhas Bank), where warm subtropical water from the Indian Ocean dominates and wind-driven upwelling is small-scale and observed only at prominent capes in summer (Schumann and Martin, 1991; Schumann, 1999). In this study, we used these indices to test for trends in upwelling in the BUS over the 1979 to 2015 period, while a companion investigation (García-Reyes et al., 2017) identifies and compares the seasonal modes of upwelling variability in the Benguela and California systems. Based on recent climate projections (Rykaczewski et al., 2015; Wang et al., 2015), we hypothesize that positive linear trends will be evident in the poleward sectors (upwelling intensification), while those in the equatorward part of the region will be negative (decreased upwelling). This hypothesis is important as it may be related to changes in distribution, community structure and abundance that have been observed in several taxa in the ecosystem, including zooplankton, fish, rock lobster, kelp and marine birds, among others (Blamey et al., 2012; Blamey et al., 2015; Crawford et al., 2015; Watermeyer et al., 2016). Additionally, we use spectral analysis (Emery and Thomson, 2001) to better describe the non-linear variability in the time series.

2. Data and methods

We evaluated and compared wind data from different long-term data sets (Figs. 1–3) to select a wind product that has the ability to represent upwelling winds across the relatively wide shelf of the BUS, and is consistent in time and space, as we are interested in evaluating upwelling variability over the long-term and comparison between regions over the larger scale. The evaluated data sets include (Table 1) output from the Fleet Numerical Meteorological and Oceanographic Center (FNMOC, http://www.usno.navy.mil/FNMOC), NCEP/NCAR Reanalysis 1 project (http://www.esrl.noaa.gov/psd/data/reanalysis/reanalysis.shtml), the NCEP-DOE Reanalysis 2 (http://www.esrl.noaa.gov/psd/data/gridded/data.ncep.reanalysis2.html), 20th Century Reanalysis version 2 (http://www.esrl.noaa.gov/psd/data/20thC_Rean), iCOADS (http://icoads.noaa.gov), ERA/ECMWF (http://www.ecmwf.int/en/research/climate-reanalysis/era-interim). Wind data from coastal stations and scatterometers have not been included in this comparison since previous studies in the Benguela region (Blamey et al., 2012, and references therein) have recently documented strong significant correlations between measured and geostrophic winds, and between scatterometer and geostrophic winds. Similarly, a recent study by Roy et al. (2016) shows very good correspondence between 20th Century Reanalysis products and winds from a coastal anemometer in the Benguela system.

The results of this comparison, discussed further in Section 3.1., show that compared with other data sets, NCEP-DOE Reanalysis 2 wind vectors (Kanamitsu et al., 2002) provide the most consistent, up-to-date, high temporal frequency data across the region (Capet et al., 2004; Cardone et al., 1990; Kent et al., 2013). Thus, daily averaged NCEP-DOE Reanalysis 2 wind vectors were used to describe upwelling variability along the Namibian and South African coasts for the period from 1 July 1979 to 30 June 2015. At each location, wind vectors were rotated to account for the orientation of the coastline and wind stress was computed using the non-linear drag coefficient defined by Large and Pond (1981) and modified by Trenberth et al. (1990) for low wind speeds. Ekman transport ($m^3\ s^{-1}$) per 100 m of coastline was then computed, with positive values indicating offshore transport

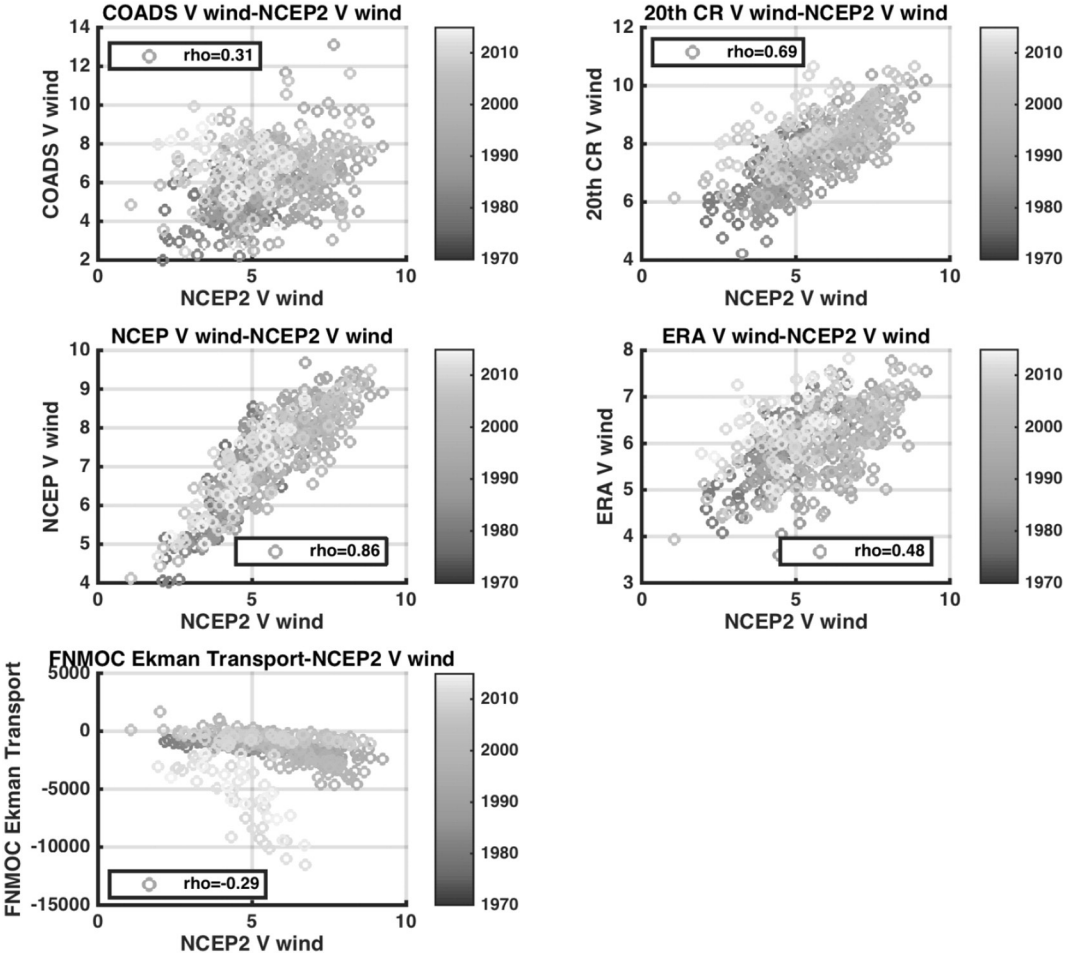

Fig. 1. Monthly meridional wind speed data from NCEP2 compared to other data sets wind speed (Offshore Ekman transport for the FNMOC model output), for the location centred at 21°S, 12°E in the northern BUS (Benguela Upwelling System) region.

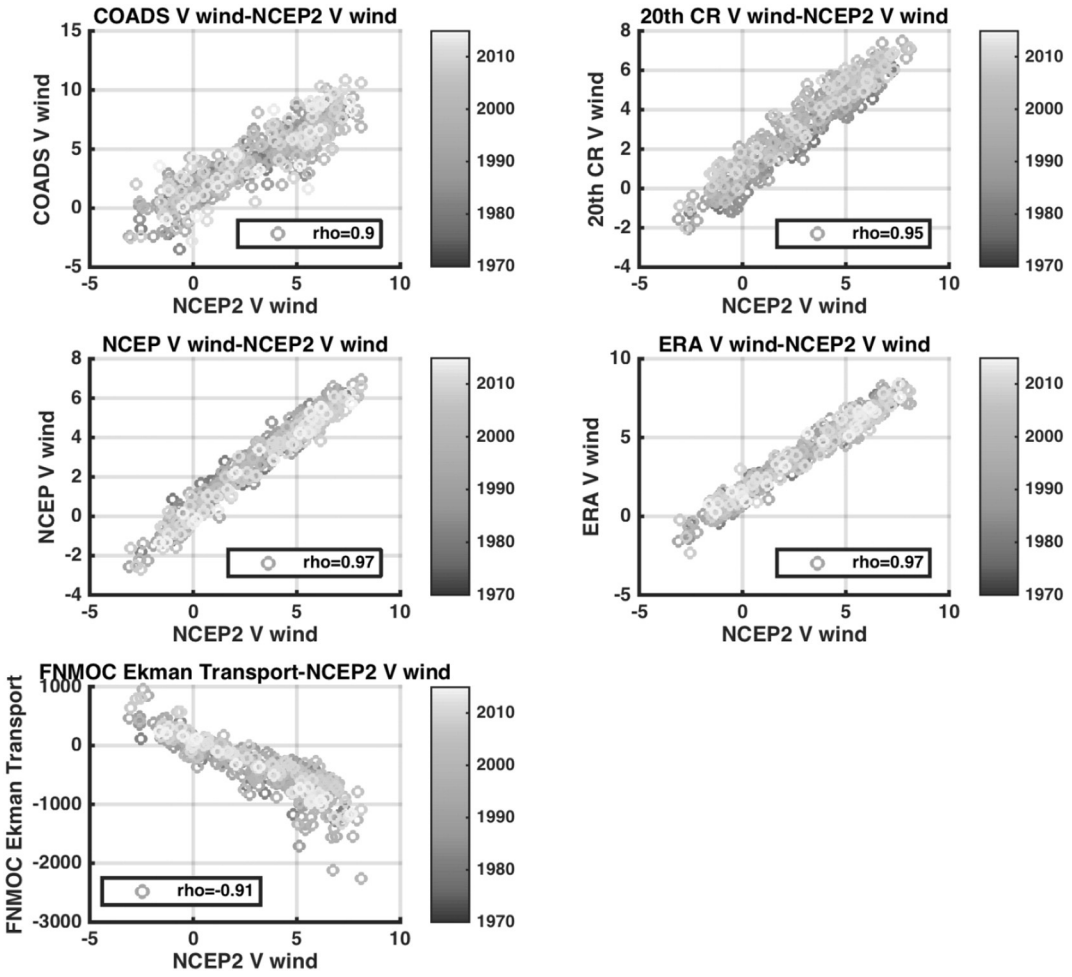

Fig. 2. Monthly meridional wind speed data from NCEP2 compared to other data sets wind speed (Offshore Ekman transport for the FNMOC model output), for the location centred at 33°S, 17°E in the southern BUS (Benguela Upwelling System) region.

(upwelling), and negative values representing onshore transport (downwelling). Similar to Roy et al. (2001) and van der Lingen et al. (2016), daily values were summed such that upwelling events were defined as periods of consecutive days of positive (offshore) Ekman transport, while downwelling events were indicated by periods of consecutive days of negative (onshore) Ekman transport (Fig. 4).

Unlike the upwelling indices developed by Schwing et al. (2006) and Bograd et al. (2009), we derive indices that quantify upwelling and downwelling variability separately. By separately integrating positive (offshore) and negative (onshore) Ekman transport, a more accurate estimation of the total amount of upwelling and the number of upwelling days is obtained, which also allows for the determination and comparison of the magnitude and influence of individual events. Since upwelling in the southern BUS is strongly seasonal, with peaks occurring during austral spring and summer (Hutchings et al., 2009), years were defined from 1 July of one year to 30 June of the following year (e.g. 1979 = 1 July 1979 to 30 June 1980), to capture the full upwelling season in a single 12-month period.

Using daily data, the following upwelling indices (Fig. 4) were computed:

(1) Total cumulative upwelling (TCU); defined as the sum of all positive (offshore) Ekman transport per year.
(2) Total cumulative downwelling (TCD); defined as the sum of all negative (onshore) Ekman transport per year.
(3) Number of upwelling days (NUD); defined as the total number of days per year on which positive (offshore) Ekman transport occurs.
(4) Number of upwelling events (NUE); defined as the total number of continuous periods of positive (offshore) Ekman transport per year.
(5) Number of downwelling days (NDD); defined as the total number of days per year on which negative (onshore) Ekman transport occurs.
(6) Number of downwelling events (NDE); defined as the total number of continuous periods of negative (onshore) Ekman transport per year.

Averages of the upwelling indices were computed per region (Fig. 4), for the northern BUS (15–29°S), southern BUS (29–36°S), and the Agulhas Bank (19–29°E), and are presented in Figs. 5–7. Results of linear and quadratic regression analyses on the upwelling indices are presented in Tables 2 and 3. Additional results on the correlations between indices within each region and among regions, as well as the regression and spectral analyses used to investigate the long-term trends, and inter-annual to decadal variations in the upwelling indices, have been included in the Supplementary Material (SM).

To investigate the South Atlantic Anticyclonic (SAH) atmospheric pressure system as a driver of wind, and hence upwelling variability, regionally-averaged annual TCU values were compared with the annual magnitude and zonal (SAHx) and meridional (SAHy) positions of the SAH. Monthly NCEP-DOE Reanalysis 2 Sea Level Pressure (SLP) was used to compute the magnitude and position of the SAH according to Schroeder et al. (2013). Based on the climatology between 1979 and 2014, the 1018 hPa isobar was used to define the SAH. The magnitude

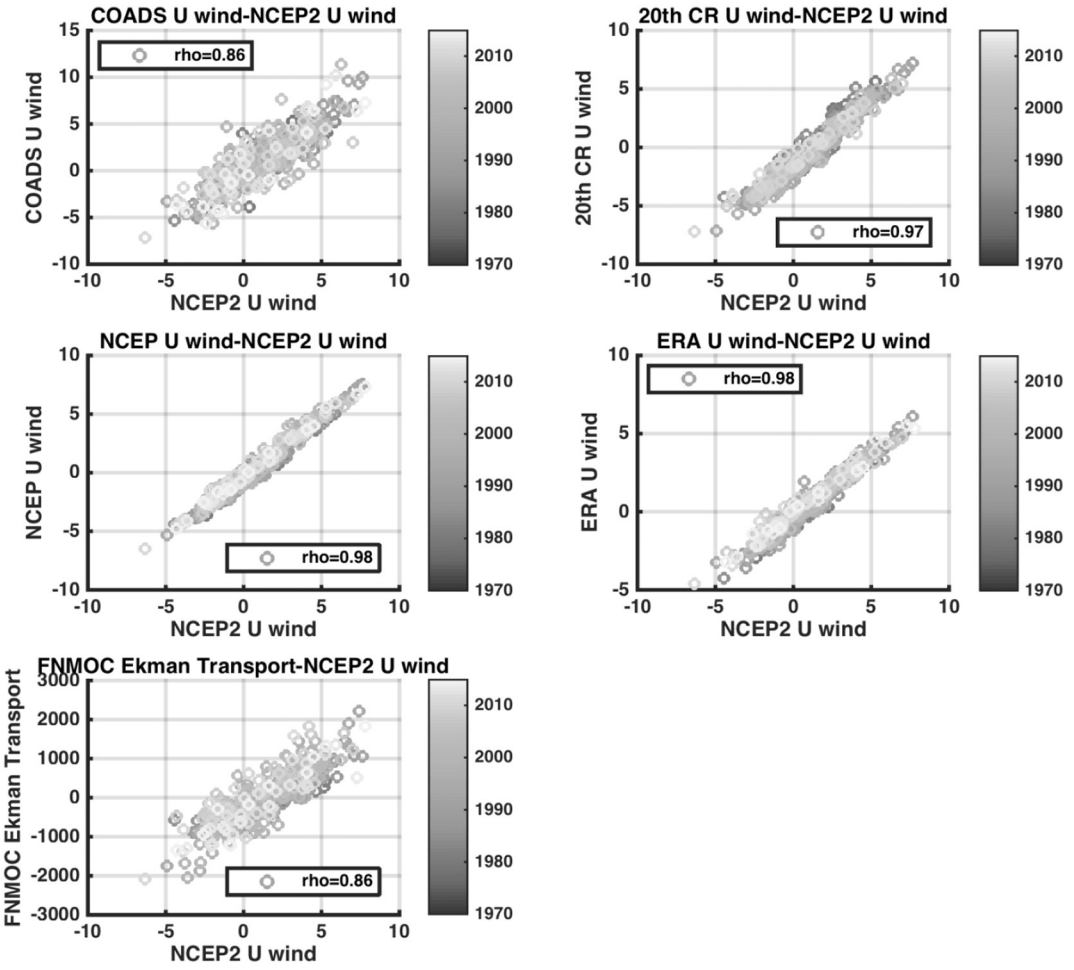

Fig. 3. Monthly zonal wind speed data from NCEP2 compared to other data sets wind speed (Offshore Ekman transport for the FNMOC model output), for the location centred at 35°S, 21°E in the Agulhas Bank region.

of the SAH was defined as the average SLP within the 1018 hPa isobar, while the position of the SAH was determined using the location of the weighted mean SLP within this isobar. Anomalies of the magnitude and position of the SAH were computed and rank-correlated with TCU in the northern and southern BUS, and on the Agulhas Bank. The difference in SLP between the centre of the SAH and the shelf region (20°S; 12.5°E for the northern BUS, 32.5°S; 17.5°E for the southern BUS, and 35°S; 22°E for the Agulhas Bank) was also investigated.

3. Results

3.1. Dataset comparison

Figs. 1–3 show scatterplots comparing monthly averaged data of NCEP-DOE Reanalysis 2 upwelling-favourable wind speed with the other data sets (Table 1) analysed for each region. In addition, Figs. SM1–SM3 show monthly averaged upwelling-favourable wind speed

Table 1
Wind data sets compared for this study.

Dataset	Period	Temporal resolution	Spatial resolution	Source
FNMOC Model Output	1981–2015	Daily	1°	USA Navy
NCEP/NCAR Reanalysis 1	1948–2015	Daily	1.88°	NOAA
NCEP-DOE Reanalysis 2	1979–2015	Daily	2.5°	NOAA
20th Century Reanalysis V2	1851–2012	Daily	2°	NOAA
iCOADS data	1960–2015	Monthly	1°	NOAA
ERA/ECMWF Reanalysis	1979–2015	Daily	80 km	ECMWF

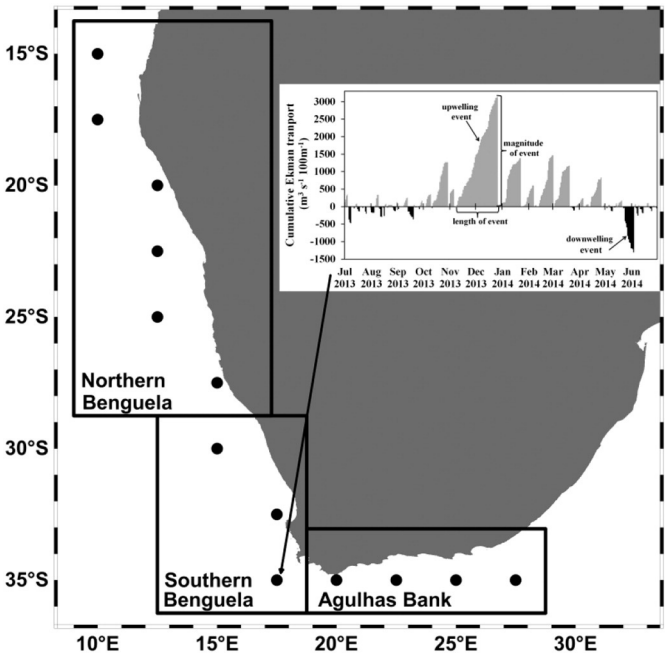

Fig. 4. Map showing regions of the Benguela Upwelling System. Inset illustrates cumulative Ekman transport off Cape Point and definition of upwelling and downwelling indices. Black dots indicate the centres of the 2.5°×2.5° data cells used.

(except for the FNMOC model output, which shows offshore Ekman transport) for each of the three regions. Overall, the largest inconsistencies between the various data sets occurred in the northern BUS, where the lowest correlations were observed (Fig. 1). Correlations of NCEP-DOE Reanalysis 2 with iCOADS and with the FNMOC data sets were the lowest (Fig. 1). Although these correlations were substantially higher in the southern BUS and Agulhas Bank regions, they were still lower than the correlations between NCEP-DOE Reanalysis 2 and other data sets in each region (Figs. 2 and 3). iCOADS showed much larger temporal variability than other data sets in each of the regions (Figs. SM1–SM3), and the poor correlations between iCOADS and NCEP-DOE Reanalysis 2 (Figs. 1–3) were likely due to this large variability as well as the monthly resolution of the iCOADS dataset. The Ekman transport from the FNMOC model showed large discontinuities, particularly in latter years, in the northern BUS region (Fig. SM1), possibly as a result of some change in model parameters in recent years. For these reasons, the iCOADS and FNMOC data sets were discarded.

Except for ERA/ECMWF, the other data sets (NCEP/NCAR, NCEP-DOE, and 20th Century) all show similar characteristics and variability, as evidenced by the substantially high correlations between them, in the southern BUS and Agulhas Bank regions (Figs. 1–3 and SM1–SM3). The highest correlations in each of the regions were observed for the NCEP/NCAR and NCEP-DOE data sets (Figs. 1–3), but the NCEP/NCAR data has known large biases in upwelling regions (Kent et al., 2013). Although ERA/ECMWF has smaller biases than NCEP/NCAR in upwelling regions (Kent et al., 2013), and showed consistency in time and space, it did not show the seasonal to interannual to decadal variability in the northern BUS shown by other data sets (Figs. SM1–SM3) and reported elsewhere (Kent et al., 2013). Thus, NCEP-DOE and 20th Century were selected as the data sets that showed the best consistency in space and time (Figs. 1–3 and SM1–SM3). However, the 20th Century data was only available until 2012, and thus NCEP-DOE was selected for further analysis, due to the availability of up-to-date data, and the consistency of the reanalysis model through time.

3.2. Upwelling variability

In each of the three regions (Figs. 5–7), all indices showed clear interannual and decadal variability, with TCU in the northern BUS (Fig. 5a) being an order of magnitude greater than that in the southern BUS (Fig. 6a), and TCU on the Agulhas Bank being two orders of magnitude lower (Fig. 7a). In the northern and southern BUS, there was significant correlation between most indices, except for total cumulative downwelling (Table SM1). In contrast, on the Agulhas Bank, fewer indices were correlated with each other (Table SM1). On the Agulhas Bank, TCU was significantly correlated only with NUD and NDD, in contrast to the northern and southern BUS (Table SM1). Significant positive correlations were observed for TCU, NUE, and NDE between the northern and

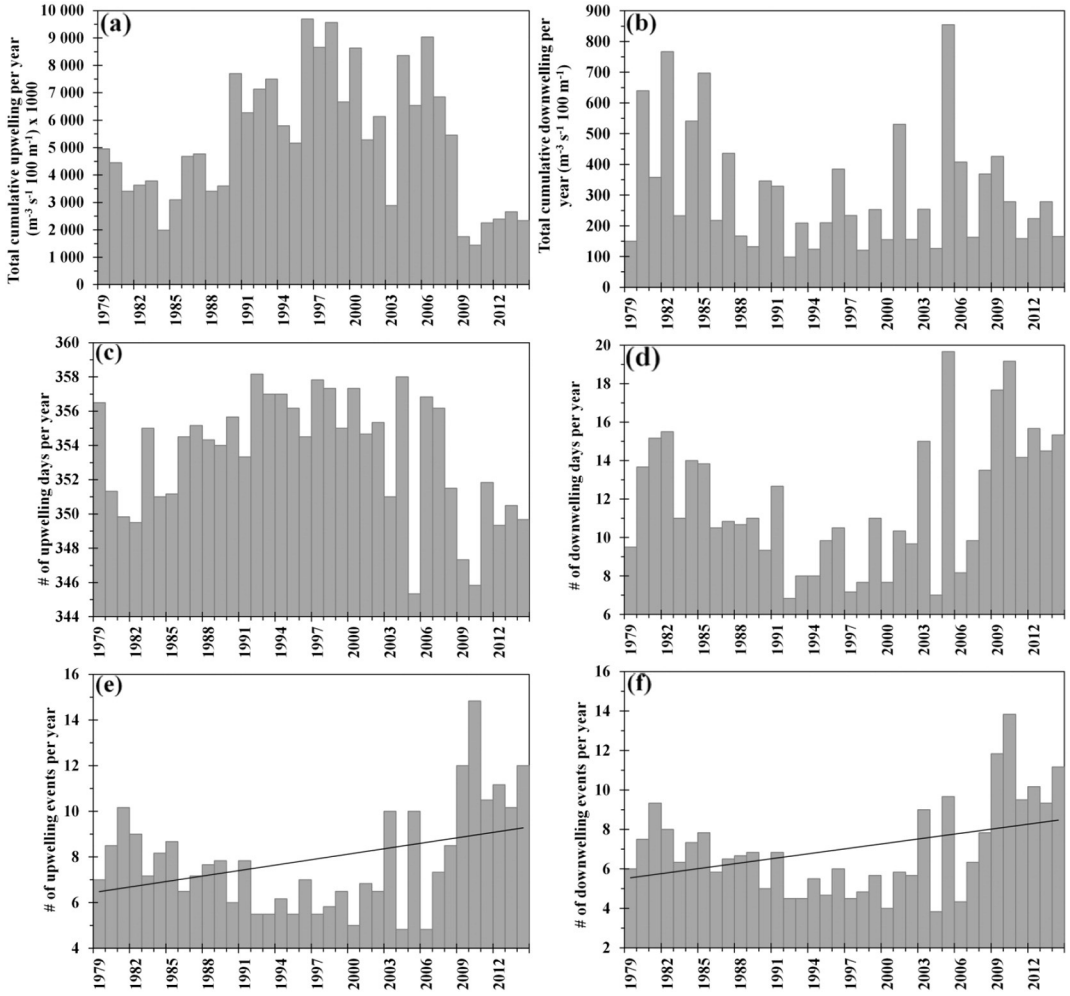

Fig. 5. Northern Benguela Upwelling System (BUS) indices, showing (a) TCU: Total cumulative upwelling per year ($m^{-3}\ s^{-1}\ 100\ m^{-1} \times 1000$), (b) TCD: Total cumulative downwelling per year ($m^{-3}\ s^{-1}\ 100\ m^{-1}$), (c) NUD: number of upwelling days per year, (d) NUD: number of downwelling days per year, (e) NUE: number of upwelling events per year, and (f) NDE: number of downwelling events per year. Solid black lines indicate the significant linear trends.

southern BUS (Table SM2). In contrast, NUD and NDD were significantly and positively correlated between the southern BUS and Agulhas Bank (Table SM2).

In the northern BUS, the highest TCU occurred between 1990 and 2008, with less upwelling in the 1980s and substantially lower upwelling between 2009 and 2014 (Fig. 5a). There was no linear trend in TCU in the northern BUS (Table 2), but a significant quadratic ($F_{2,33}$ = 13.322, $p < 0.001$, $R^2 = 0.447$) trend was observed (Tables 3 and SM4). In particular, between 2009 and 2014, TCU had reduced to less than half the value of the long-term mean (5.22E + 06 m^{-3} s^{-1} 100 m^{-1}) (Fig. 5a). There was no significant change in the total cumulative downwelling and the number of downwelling days in this region, and the significance of the linear increase in the number of downwelling events was likely due to autocorrelation in the time series (Fig. 5b, d, f and Tables 2, 3, SM3, SM4). Upwelling in the northern BUS is strongly perennial, where the number of upwelling days ranged between 345 and 358 days (Fig. 5c), while the number of upwelling events varied from 5 to 15 (Fig. 5e). Interestingly, 2005 and 2010 both showed the lowest number of upwelling days and the largest number of downwelling days per year (Fig. 5c, d). In 2010, this occurred in conjunction with the largest number of upwelling and downwelling events (Fig. 5e, f) and this greater variability resulted in the lowest TCU for the time series (Fig. 5a). In contrast, during 2005, there was less variability (Fig. 5e, f), and TCU was well above the long-term mean (Fig. 5a).

Larger amounts of upwelling (Fig. 5a) are generally associated with a greater number of upwelling days (Fig. 5c) and fewer events per year (Fig. 5e), while the reverse is true for smaller amounts of upwelling. This is also illustrated by the strong positive correlations between TCU and the number of upwelling days, and the strong negative correlations between TCU and the number of upwelling events (Table SM1). While the number of upwelling events showed a significant quadratic ($F_{2,33} = 19.277$, $p < 0.001$, $R^2 = 0.539$) trend (Table 3), simulation analyses (Table SM4) suggested that the significance of the linear trend was likely due to autocorrelation in the time series. Similarly, the number of upwelling days showed a significant quadratic ($F_{2,33} = 10.094$, $p < 0.001$, $R^2 = 0.380$) trend (Tables SM3 and SM4).

In the southern BUS, TCU was lowest during the 1980s and early 1990s and highest during the mid- to late 1990s (Fig. 6a). In particular, before 1995, only a few years showed TCU values above the long-term mean (4.95E + 05 m^{-3} s^{-1} 100 m^{-1}), while after 1995 there were many more years with TCU exceeding the long-term mean (Fig. 6a). Linear and quadratic trends in TCU were weak and not significant (Tables 2, 3, SM3, SM4). Offshore Ekman transport occurred, on average, for more than three quarters (267–310 days) of the year (Fig. 6c), and translated into more than twice the number of upwelling events per year (Fig. 6e),

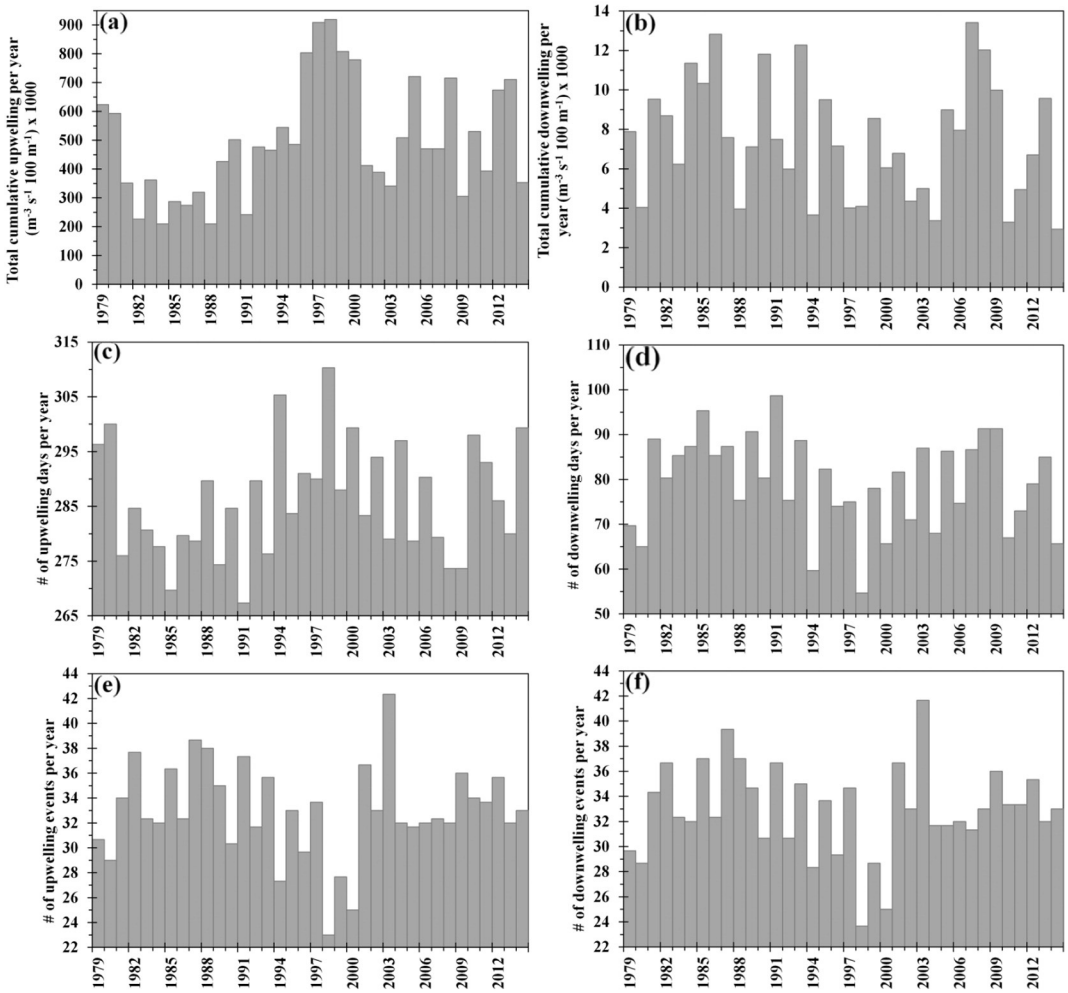

Fig. 6. Southern Benguela Upwelling System (BUS) indices, showing (a) TCU: Total cumulative upwelling per year (m^{-3} s^{-1} 100 m^{-1} × 1000), (b) TCD: Total cumulative downwelling per year (m^{-3} s^{-1} 100 m^{-1}), (c) NUD: number of upwelling days per year, (d) NUD: number of downwelling days per year, (e) NUE: number of upwelling events per year, and (f) NDE: number of downwelling events per year.

compared to the northern BUS (Fig. 5e). Similarly, the number of downwelling days and events in the southern BUS (Fig. 6d, f) was substantially higher than that in the northern BUS (Fig. 5d, f). Other upwelling indices (TCD, NUE, NUD, NDE, NDD) also showed no significant trends in the southern BUS (Tables 2–3 and SM4), likely due to substantial autocorrelation in most of the southern BUS indices, more so than in the other regions (Table SM3).

In contrast, TCU on the Agulhas Bank showed an overall increasing trend, with periods of elevated upwelling during the early to mid-1980s, the mid-1990s to early 2000s, and between 2007 and 2014 (Fig. 7a). TCU showed a significant linear increase ($F_{1,34} = 8.358$, $p = 0.007$, $R^2 = 0.197$) trend (Tables 2 and SM4), with more years exceeding the long-term mean (3.06E + 04 m^{-3} s^{-1} 100 m^{-1}) in the latter part of the time series (Fig. 7a). While substantial autocorrelation was observed in all the indices for the northern and southern BUS, there was very little autocorrelation in the Agulhas Bank indices (Table SM3). Since 1993, there have been consistently more upwelling days per year, with most years exceeding the long-term mean (163 days) (Fig. 7c). The linear trend ($F_{1,34} = 11.855$, $p = 0.002$, $R^2 = 0.259$) in NUD was also significant (Tables 2 and SM4). In contrast, the NDD (Fig. 7d) showed as a significant linear decrease (Table 2).

TCD on the Agulhas Bank (Fig. 7b) was orders of magnitude greater than that in both the southern and northern BUS (Figs. 5b and 6b), but showed no significant trends (Tables 2–3, and SM3-SM4). The number of upwelling and downwelling events on the Agulhas Bank (Fig. 7e, f) was much greater than that in the southern BUS (Fig. 6e, f). Notably, anomalously high TCU (>3 s.d.) and NUD were observed during 2010, while 2013 exhibited anomalously large values of TCD. However, both the linear and quadratic regressions remain significant when replacing these anomalously high values with the lower values from either the preceding or subsequent years.

Anomalies in the magnitude and position of the SAH showed significant linear trends (Fig. 8a, b, c), but quadratic trends (not shown) were not significant. During the early part of the time series, anomalies in the magnitude were more negative, while those in later years were more positive, indicating an overall increase in the magnitude of the sea level pressure in the centre of the SAH (Fig. 8a). The zonal (SAHx) and meridional (SAHy) positions of the SAH both showed a change from more positive anomalies in the 1980's to increasingly more negative anomalies in later years, reflecting a long-term westward and southward movement of the centre of the SAH (Fig. 8b, c). In contrast to the centre of the SAH, sea level pressure in the northern and southern BUS, and Agulhas Bank shelf regions all showed significant linear decreases over time (Fig. 8d, e, f), and while the quadratic trends in the southern BUS and Agulhas Bank regions were not significant, sea level pressure in the northern BUS also showed a significant quadratic trend (Fig. 8d, e, f). The long-term increase in SLP in the centre of the SAH and long-term decreases in the SLP in the shelf regions signifies a

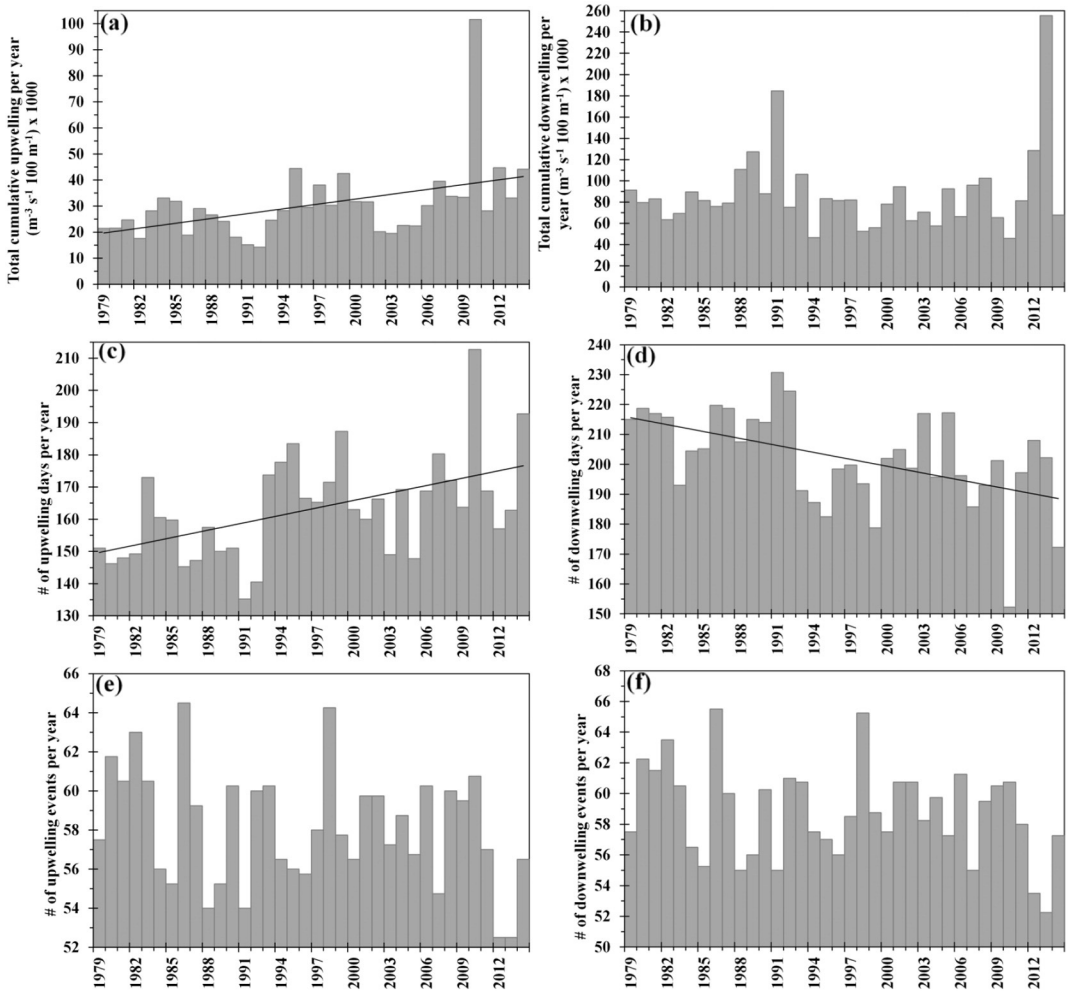

Fig. 7. Agulhas Bank indices, showing (a) TCU: Total cumulative upwelling per year (m^{-3} s^{-1} 100 m^{-1} × 1000), (b) TCD: Total cumulative downwelling per year (m^{-3} s^{-1} 100 m^{-1}), (c) NUD: number of upwelling days per year, (d) NUD: number of downwelling days per year, (e) NUE: number of upwelling events per year, and (f) NDE: number of downwelling events per year. Solid black lines indicate the significant linear trends.

Table 2
Linear regression analysis results for each of the upwelling indices in the Northern BUS (NB), Southern BUS (SB), and Agulhas Bank (AB) regions; Total Cumulative upwelling per year (TCU), Total Cumulative Downwelling per year (TCD), Number of upwelling events per year (NUE), Number of upwelling days per year (NUD), Number of downwelling events per year (NDE), and Number of downwelling days per year (NDD). $F_{1,34}$ indicates the F-statistic and the degrees of freedom. Significant regressions are shaded in grey.

Region	Index	Coefficients	$F_{1,34}$	p	R^2
NB	TCU	m = -5477	0.019	0.890	0.001
	TCD	m = 4.102	1.780	0.191	0.050
	NUE	m = 0.080	4.996	0.032	0.128
	NUD	m = -0.083	2.233	0.144	0.062
	NDE	m = 0.083	5.342	0.027	0.136
	NDD	m = 0.079	2.096	0.157	0.058
SB	TCU	m = 6028.134	3.786	0.060	0.100
	TCD	m = 47.325	0.949	0.337	0.027
	NUE	m = -0.008	0.017	0.897	0.001
	NUD	m = 0.147	0.780	0.383	0.022
	NDE	m = -0.005	0.006	0.938	0.000
	NDD	m = -0.150	0.804	0.376	0.023
AB	TCU	m = 619.753	8.358	0.007	0.197
	TCD	m = -431.237	0.474	0.496	0.014
	NUE	m = -0.079	2.860	0.100	0.078
	NUD	m = 0.769	11.855	0.002	0.259
	NDE	m = -0.077	2.580	0.117	0.071
	NDD	m = -0.773	12.012	0.001	0.261

Table 3
Quadratic regression analysis results for each of the upwelling indices in the Northern BUS (NB), Southern BUS (SB), and Agulhas Bank (AB) regions; Total Cumulative upwelling per year (TCU), Total Cumulative Downwelling per year (TCD), Number of upwelling events per year (NUE), Number of upwelling days per year (NUD), Number of downwelling events per year (NDE), and Number of downwelling days per year (NDD). $F_{2,33}$ indicates the F-statistic and the degrees of freedom. Significant regressions are shaded in grey.

Region	Index	Coefficients	$F_{2,33}$	p	R^2
NB	TCU	m_1 = 6.58E+07, m_2 = -16491	13.322	<0.001	0.447
	TCD	m_1 = 1496, m_2 = -0.374	1.538	0.230	0.085
	NUE	m_1= -61.221, m_2 = 0.015	19.277	<0.001	0.539
	NUD	m_1 = 80.821, m_2 = -0.020	10.094	<0.001	0.380
	NDE	m_1 = -61.650, m_2 = 0.015	19.146	<0.001	0.537
	NDD	m_1 = -80.931, m_2 = 0.020	10.339	<0.001	0.385
SB	TCU	m_1 = 1.71E+06, m_2 = -425.719	2.759	0.078	0.143
	TCD	m_1 = 2636.181, m_2 = -0.648	0.468	0.630	0.028
	NUE	m_1 = -19.700, m_2 = 0.005	0.274	0.762	0.016
	NUD	m_1 = 3.407, m_2 = -0.001	0.379	0.687	0.022
	NDE	m_1 = -13.331, m_2 = 0.003	0.135	0.874	0.008
	NDD	m_1 = -3.518, m_2 = 0.001	0.391	0.679	0.023
AB	TCU	m_1 = -9.77E+04, m_2 = 24.617	4.767	0.015	0.224
	TCD	m_1 = 3.17E+05, m_2 = -79.528	0.942	0.400	0.054
	NUE	m_1 = 5.182, m_2 = -0.001	1.424	0.255	0.079
	NUD	m_1 = 0.065, m_2 = 0.000	5.753	0.007	0.259
	NDE	m_1 = 11.614, m_2 = -0.003	1.421	0.256	0.079
	NDD	m_1 = -0.176, m_2 = 0.000	5.829	0.007	0.261

long-term increase in the SLP difference between the SAH and shelf regions.

Correlations between TCU and the magnitude and zonal position of the SAH were not significant (Fig. 9). TCU in the southern BUS and Agulhas Bank regions showed significant negative correlations with the meridional position of the SAH (Fig. 9), indicating the occurrence of more upwelling-favourable wind in these regions when the SAH was located further south. Since TCU on the Agulhas Bank during 2010 was identified as an outlier, we computed the correlations with and without the 2010 value, but the results did not change with regard to the relationship or the significance of the correlations. For the northern BUS, the correlation with the meridional position of the SAH was also negative (Fig. 9), but was not significant. Similarly, the correlations between TCU and the sea level pressure difference in each of the regions was also significant (Fig. 9), with larger amounts of upwelling associated with greater SLP differences. The SLP difference in each of the regions showed significant correlations with the magnitude and position of the SAH (Fig. 10). Elevated SLP differences were associated with increases in the magnitude, and with negative anomalies in the zonal and meridional positions of the SAH (Fig. 10).

4. Discussion

In the Benguela Upwelling System, as in many regions of the world, systematic, high-resolution, wide-coverage, long-term data sets of meteorological and oceanographic measurements are lacking. Global model output, reconstructions and reanalysis data sets are solutions to this problem and provide data when none or only sparse data is available. While the decision to base the current study on reanalysis products was motivated by the lack of regional wind measurements, whether in situ or satellite, with sufficient spatial coverage and adequate temporal resolution to identify long-term trends and variations, it must be kept in mind that the trends and variability described using these products are dependent on their quality and homogeneity of the reanalysis models. Large differences in wind stress trend estimates have been observed from different reanalysis, as well as observational, data sets (Narayan et al., 2010). However, our results (Figs. 1–3) show that there is good consistency between some of these reanalysis products, particularly in the southern BUS and Agulhas Bank regions.

Intrinsic long-term bias (Cardone et al., 1990) and coarse resolution (Kent et al., 2013) are among the caveats commonly discussed for these data sets. For regions, such as the southern Hemisphere, bias can be exacerbated by the lack of local in situ data to validate, adjust and correct models and reconstructions (Backeberg et al., 2012). Additionally, for upwelling regions, the resolution provided by such data sets (in space and time) might be too coarse to adequately represent the coastal, synoptic nature of upwelling winds and events (Capet et al., 2004; Kent et al., 2013). It is also important to recognise that due to their coarse resolution, reanalysis products also do not account for the small-scale effects of sea surface temperature and ocean currents on wind stress and wind stress curl (Chelton et al., 2004; Risien and Chelton, 2008), but it is not clear if these limitations have an effect on the long-term trends in wind stress (Tim et al., 2015). Since the focus of the current study is to investigate and describe the long-term trends in upwelling-favourable winds, it requires the use of data with the longest possible timescale. This necessitates a trade-off between datasets with the longest timescales and those with higher resolution and quality. However, it should also be noted that given the temporal and spatial scales of variability in both climate and ecosystems, higher resolution wind data (in space or time) does not necessarily help to improve the relationships between climate variability and ecosystem responses, as seen in the California Current system (Black et al., 2011; García-Reyes et al., 2013).

A previous study by Chen et al. (2012) defined upwelling indices based on sea surface temperature (SST) and offshore Ekman transport, and concluded that while the SST-based index provided a good representation of the spatial variation of upwelling, the offshore Ekman

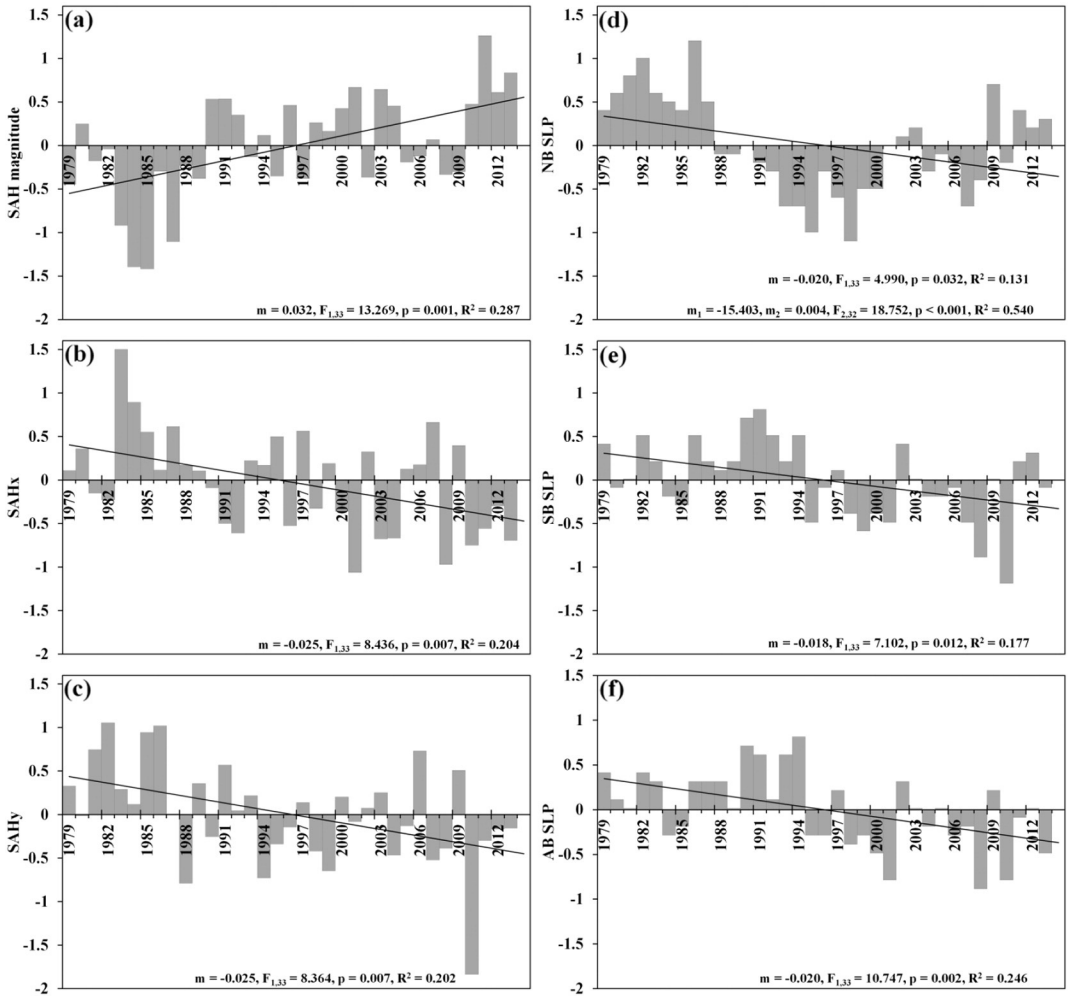

Fig. 8. Anomalies of the (a) magnitude, (b) zonal position (SAHx), and (c) meridional position (SAHy) of the South Atlantic Anticyclonic pressure system, and anomalies of sea level pressure (SLP) at selected locations in the (d) northern BUS (NB; 20°S; 12.5°E), (e) southern BUS (SB; 32.5°S; 17.5°E), and (f) Agulhas Bank (AB; 35°S; 22°E). Solid black lines indicate the significant linear trends.

transport-based index was more appropriate for evaluating temporal variations of upwelling intensity in the Benguela upwelling system. While the indices presented here provide a good assessment of the temporal variations in upwelling driven by Ekman transport, it is important to recognise that, in addition to Ekman transport, there are several other mechanisms which also result in upwelling. Upwelling is also driven by the cyclonic curl of the wind stress, which can be a significant source of nutrients in coastal ecosystems (Rykaczewski and Checkley, 2008). Although the rate of upwelling by Ekman transport is an order of magnitude greater than that of curl-driven upwelling (Rykaczewski and Checkley, 2008), it has been shown that, on average, curl-driven upwelling contributes 23% of the total volume of upwelled waters in the Benguela region (Messié et al., 2009). However, it has been suggested that upwelling induced by Ekman transport is more important to ecosystem functioning in coastal ecosystem than curl-driven upwelling, as it uplifts deeper waters with higher nutrient concentrations into the euphotic zone (Chavez and Messié, 2009).

Upwelling can also be enhanced or suppressed by cross-shore geostrophic currents, but this mechanism is often overlooked because of the relatively weak magnitudes of these flows (Colas et al., 2008; Marchesiello and Estrade, 2010; Marchesiello et al., 2010; Oerder et al., 2015). In the Benguela system, Veitch et al. (2010) showed that in the northern part of the system, convergence due to onshore geographic flow inhibits upwelling, while in the southern part, geostrophic divergence results in enhanced upwelling. Furthermore, Chavez and Messié (2009) have demonstrated that the Benguela region is dominated by high intraseasonal variability driven by local mesoscale activity, which shows weak seasonal and strong interannual variability (Chaigneau et al., 2009). This mesoscale activity has been shown to limit the offshore extent of upwelled waters (Chen et al., 2012), and is also known to reduce productivity in coastal upwelling systems by the subduction and offshore transport of nutrient-rich waters (Gruber et al., 2011; Rossi et al., 2008).

Nevertheless, the focus of the current study was to describe the long-term variations in upwelling driven by offshore Ekman transport, as opposed to the total upwelling from all processes, and the indices defined here and applied to the BUS show spatial heterogeneity and regional characteristics in agreement with previous descriptions of upwelling variability (Hutchings et al., 2009). The northern BUS exhibits perennial upwelling (>95% of the year, on average), approximately an order of magnitude greater than in the southern BUS, where upwelling exhibits stronger seasonality but occurs during most (>75%) of the year. The Agulhas Bank region exhibits the strongest downwelling of all the regions, and upwelling conditions for <50% of the year. In addition to the differences in the annual magnitude of upwelling, temporal trends in upwelling also varied regionally over the 1979–2015 period. Strong inter-decadal variability was observed in all regions (confirmed by spectral analysis – see Figs. SM5–SM7). Most notably, in all the regions,

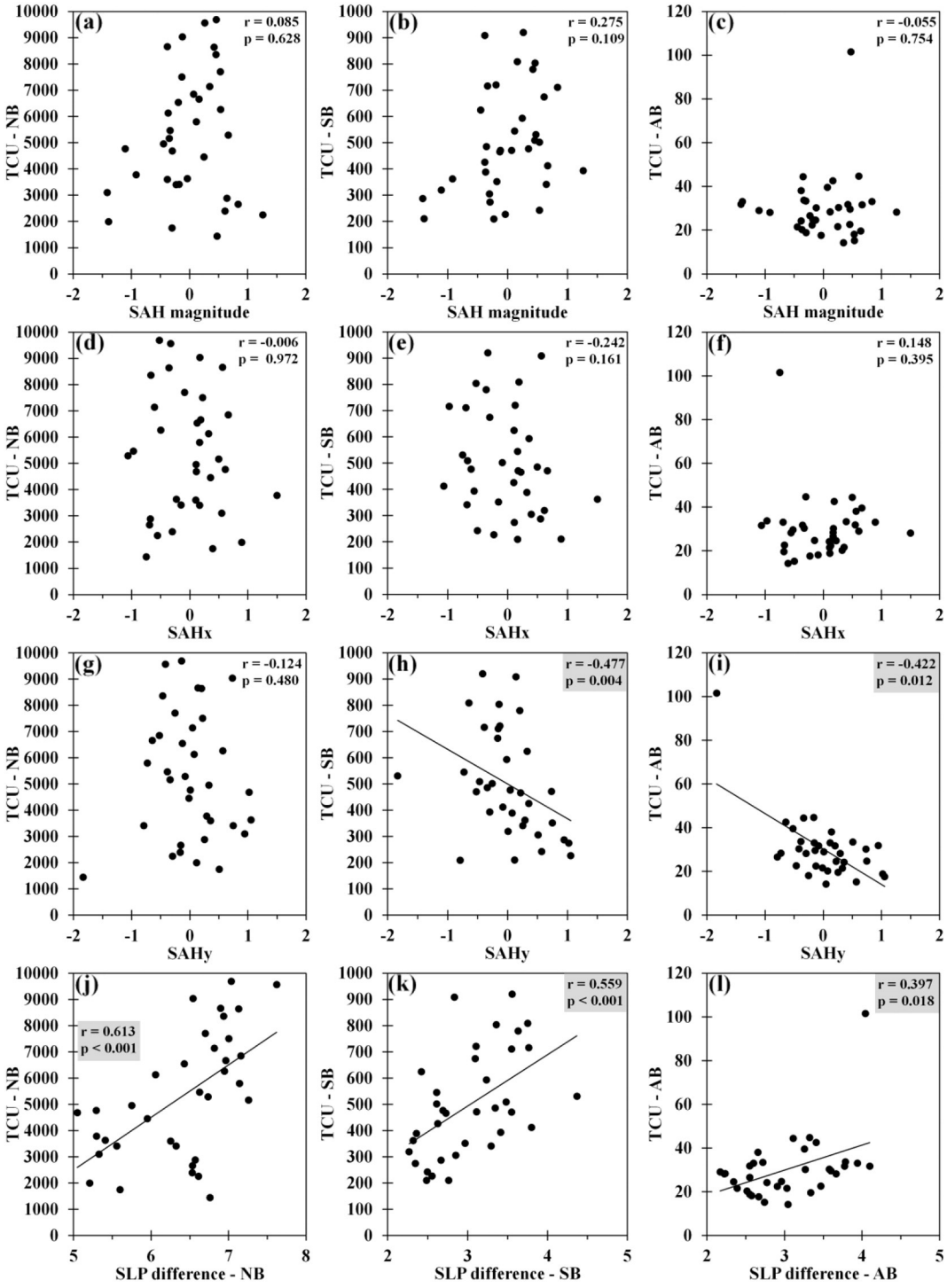

Fig. 9. Scatterplots showing Spearman correlations (r) and significance (*p*-values) between the (a, b, c) anomalies of the magnitude of the South Atlantic Anticyclonic (SAH) atmospheric pressure system, (d, e, f) anomalies of the zonal position (SAHx), (g, h, i) anomalies of the meridional position (SAHy) of the SAH, and (j, k, l) sea level pressure (SLP) differences, and Total Cumulative Upwelling (TCU) in the northern BUS (NB), southern BUS (SB), and Agulhas Bank (AB) regions. Significant correlations are indicated by solid black lines and grey shading.

the strongest variability was observed at periods of 2.01–2.54 years, and those > 14 years (Figs. SM5–SM7). In contrast to the northern (Fig. SM5) and southern BUS (Fig. SM6), the Agulhas Bank showed additional strong variability at periods of 4.92–5.82 years (Fig. SM7).

Despite the inter-decadal variability, there was an overall intensification of upwelling along the Agulhas Bank, and although the trend was not significant, there was a tendency toward increased upwelling in the southern BUS. While there was no significant long-term trend in TCU in the northern BUS, upwelling in recent years (2009–2015) has been substantially lower. These trends are associated with changes in the number of days of upwelling in each region, with a significant increase in upwelling days on the Agulhas Bank and an increasing tendency of this in the southern BUS, and a trend toward fewer days (and more episodic upwelling events, as upwelling has become less continuous) in the northern BUS in recent years.

These observations update and confirm the meta-analysis of Sydeman et al. (2014), in which subtle and spatially variable changes in upwelling, particularly in the poleward realms of EBUEs were

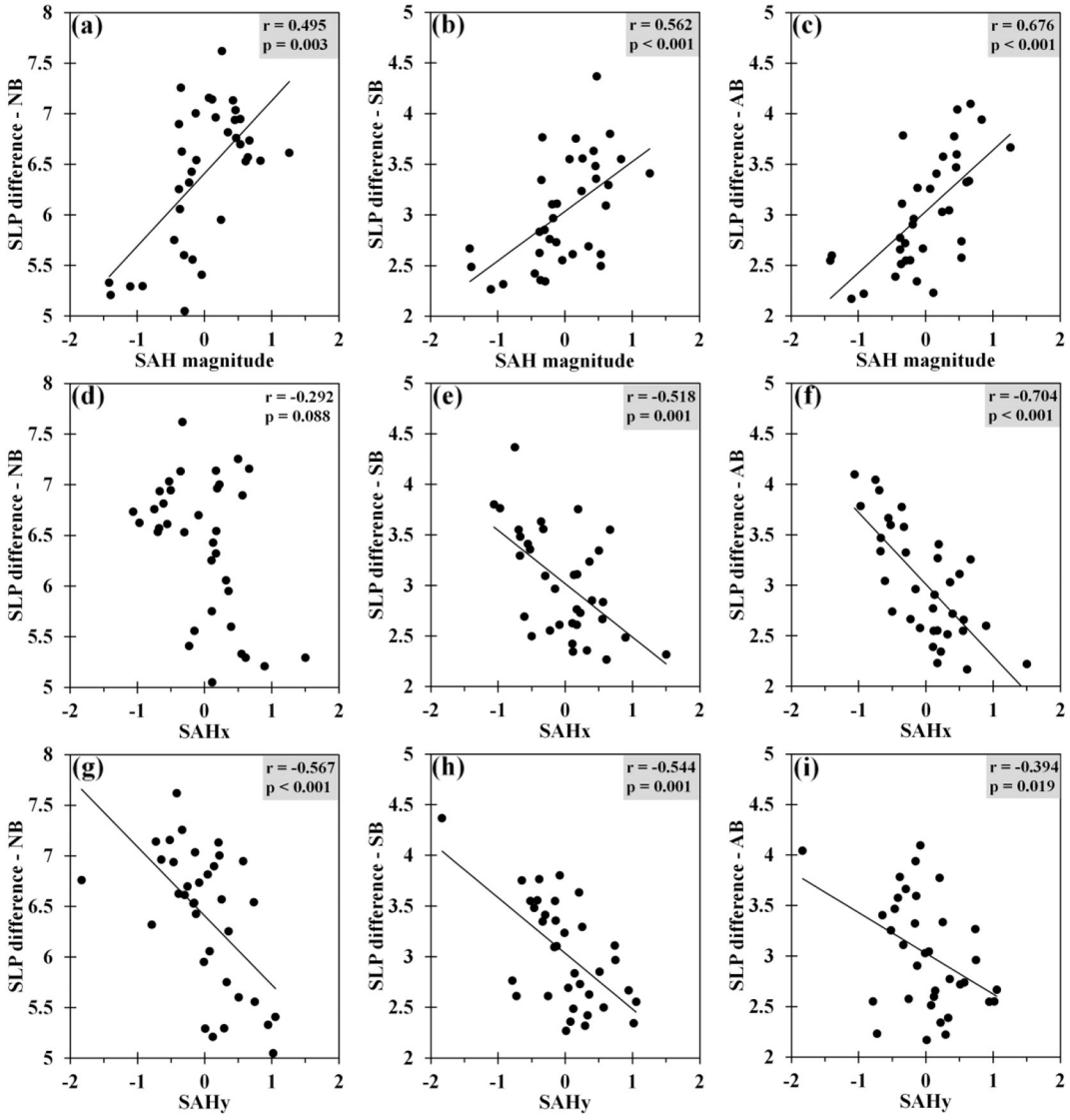

Fig. 10. Scatterplots showing Spearman correlations (r) and significance (*p*-values) between the (a, b, c) anomalies of the magnitude of the South Atlantic Anticyclonic (SAH) atmospheric pressure system, (d, e, f) anomalies of the zonal position (SAHx), (g, h, i) anomalies of the meridional position (SAHy) of the SAH, and sea level pressure (SLP) differences in the northern BUS (NB), southern BUS (SB), and Agulhas Bank (AB) regions. Significant correlations are indicated by solid black lines and grey shading.

suggested. Although the recent changes in upwelling noted here are present over short time scales (roughly 10 to 30 years) relative to the inter-decadal and centennial time scales necessary to document changes associated with anthropogenic forcing, the observed changes are consistent with modeling results that predict future upwelling intensification in the poleward portions of EBUEs (Rykaczewski et al., 2015; Wang et al., 2015). Furthermore, in comparison to previous studies, these indices show how changes in upwelling are related to synoptic-scale variations in upwelling and downwelling conditions, and provide a refined understanding of the trends, be they unidirectional or inter-decadal in nature.

The decline in TCU in the northern BUS since 2006 corresponds with the positive linear trends identified in sea surface temperature (SST) in this region (Jarre et al., 2015). Similarly, the observed variations in upwelling in the southern BUS and on the Agulhas Bank are consistent with SST fluctuations and coastal cooling (Rouault et al., 2010, Roy et al., 2007). Our study also illustrates a possible change-point in upwelling across all regions in the mid- to late-2000s; the decrease in upwelling in the northern BUS occurred in 2008/2009, as did a change in the number of downwelling and upwelling days (2009/2010) and total cumulative downwelling (2004/2005) in the southern BUS. In this regard, one of the most surprising findings was the extraordinarily strong upwelling observed along the Agulhas Bank in 2010. This spike in upwelling was >3 s.d. above the mean for the region and we question its accuracy. However, this spike in upwelling is associated with the most southerly location of the SAH (Fig. 8c), and other data sources also demonstrate a major shift in conditions in this year (see SM), so we consider that data point reliable.

The annual to multi-decadal variations in upwelling-favourable winds along the west coast are associated with shifts in the magnitude (García-Reyes et al., 2013), and meridional position (Hutchings et al., 2009; Jarre et al., 2015; Rykaczewski et al., 2015) of the atmospheric South Atlantic Anticyclone (SAH). Changes in TCU were more strongly correlated with meridional than with zonal excursions of the SAH (Fig. 9). And although westerly and southerly excursions of the SAH were associated with larger differences in sea level pressure between the SAH and the shelf in each of the regions (Fig. 10), the larger distance between the SAH and the shelf in the northern BUS served to decrease the pressure gradient there, resulting in decreased TCU. In the southern BUS and Agulhas Bank regions, higher TCU, and hence more upwelling-favourable wind, was observed when the SAH was located further south.

While the Agulhas Current, which flows along the Agulhas Bank shelf edge, is known to uplift cold nutrient-rich water onto the shelf

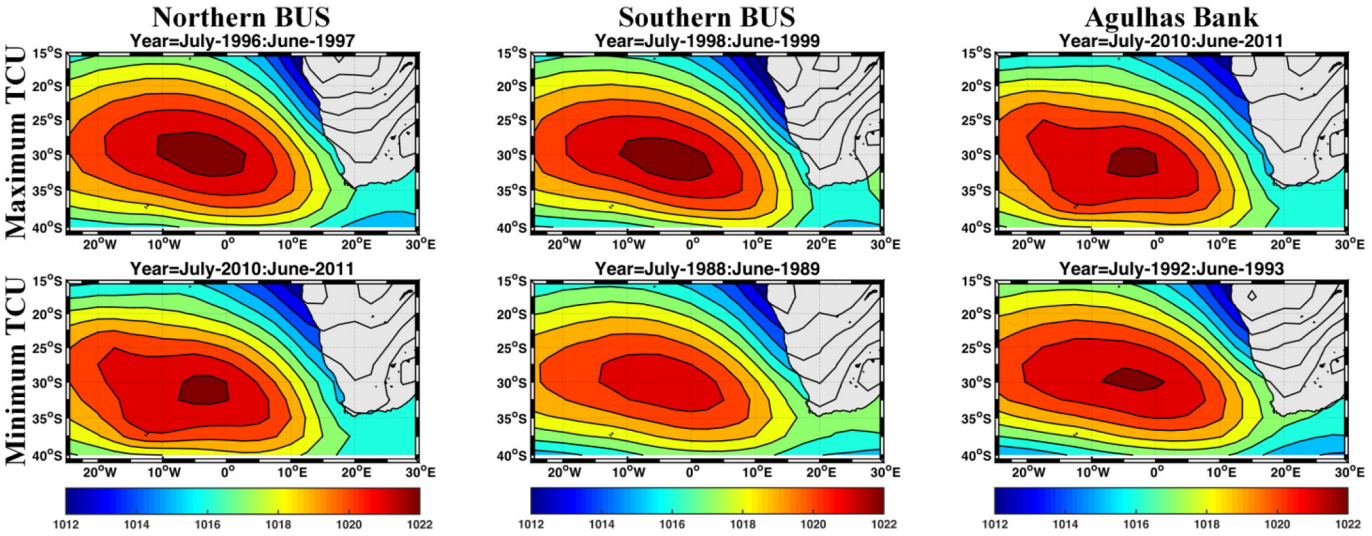

Fig. 11. Annual average sea level pressure (SLP, hPa) maps showing the magnitude and position of the South Atlantic Anticyclonic pressure system during years of minimum and maximum upwelling (TCU) in the northern BUS, southern BUS, and Agulhas Bank.

through Ekman veering, it has been shown the Agulhas Current has a limited influence at the coast, except on the far eastern side (east of 25°E) where the shelf is much narrower and plumes of warm Agulhas Current water are frequently advected into the bay (Goschen et al., 2012; Schumann, 1998, 1999). Although the Agulhas Bank is located further east of the SAH than the northern and southern Benguela subsystems, it is well-established that wind-driven upwelling occurs along this coast (Schumann et al., 1982, 1988; Walker, 1986), and that the upwelling-favourable winds are associated with the south-eastward ridging of the SAH (Schumann et al., 1995). These patterns are clearly illustrated for minimum and maximum TCU in each of the regions (Fig. 11), and these changes in upwelling and the position of the SAH are in agreement with the shifts in the SAH described by Jarre et al. (2015). Similar observations of increased upwelling-favourable wind stress in the southern Benguela and Agulhas Bank regions have been made by Tim et al. (2015), and they attributed this to a positive pressure anomaly south of the continent, rather than the intensification of the SAH. However, it is likely that this positive pressure anomaly south of the continent is a result of the long-term southward migration of SAH, as illustrated in Fig. 8c.

Interestingly, there appears to be no relationship between TCD (downwelling) indices and changes in the magnitude and position of the SAH (correlations not shown). However, there have been no comparable analyses of the long-term variations in downwelling, nor its drivers, since most of the previous work has inferred downwelling from the lack of upwelling at the event-scale, or focussed on deviations from climatological mean patterns (Roy et al., 2001; van der Lingen et al., 2016). The lack of correlation between the amount of upwelling and downwelling in all of the regions suggests that both wind direction and wind speed are changing over time in relation to changes in the magnitude and position of the SAH.

These upwelling indices should help to better understand drivers of environmental change in the BUS and other EBUEs. For example, while the yield of pelagic fisheries in the southern BUS has remained relatively constant (Hutchings et al., 2009), there has been a pronounced eastward re-distribution of pelagic resources, of anchovy in particular, from the southern Benguela to the Agulhas Bank, which could be related to changes in upwelling (Roy et al., 2007). While the eastward shift has persisted for anchovy adults, the distributional change shown by sardine has not, likely as a result of fishing pressure impacting more strongly on sardine distribution (Coetzee et al., 2008). This anchovy shift in the mid-1990s was associated with a change in the annually averaged wind speed (Roy et al., 2007), but our indices indicate that rather than a change in total upwelling occurring by means of changed wind speed only, there was also a change in the number of upwelling days in the region during this period.

Changes in upwelling and forage fish distribution may also explain regional population trends, in marine wildlife, in particular several bird species reliant upon pelagic fish for sustenance, particularly from the early- to mid-1990s. Some seabirds (e.g. Cape Gannets) also appear to have re-distributed to the Agulhas Bank (Blamey et al., 2012; Blamey et al., 2015; Crawford et al., 2015). Similarly, changes in upwelling may also be partly responsible for population shifts (decline, in this case) of pelagic resources in the California upwelling system (MacCall et al., 2016; Zwolinski and Demer, 2012). Application of these upwelling indices to biological time series in these systems will provide insight into upwelling-ecosystem relationships and how the Benguela and other EBUE systems are similar or different in their responses to climate change and variability.

Acknowledgements

NCEP-DOE Reanalysis 2 data was provided by the NOAA/OAR/ESRL PSD, Boulder, Colorado, USA (http://www.esrl.noaa.gov/psd/). The authors thank the Department of Environmental Affairs (DEA) and the Department of Agriculture, Forestry and Fisheries (DAFF), South Africa for funding and facilities. MGR, SJB, and WJS were funded by the NSF award No: OCE-1434732. The authors also express sincere thanks to Dr. Stephen Kirkman (DEA, South Africa) and Dr. Ryan Rykaczewski (University of South Carolina) for invaluable discussions and comments.

Appendix A. Supplementary data

Supplementary data to this article can be found online at http://dx.doi.org/10.1016/j.jmarsys.2017.05.007.

References

Backeberg, B.C., Penven, P., Rouault, M., 2012. Impact of intensified Indian Ocean winds on mesoscale variability in the Agulhas system. Nat. Clim. Chang. 2:608–612. http://dx.doi.org/10.1038/NCLIMATE1587.

Bakun, A., 1973. Coastal upwelling indices, West Coast of North America, 1946-71. NOAA Tech. Rep. (NMFS SSRF-671, 114 pp).

Black, B.A., Schroeder, I.D., Sydeman, W.J., Bograd, S.J., Wells, B.K., Schwing, F.B., 2011. Winter and summer upwelling modes and their biological importance in the California Current Ecosystem. Glob. Chang. Biol. 17:2536–2545. http://dx.doi.org/10.1111/j.1365-2486.2011.02422.x.

Blamey, L.K., Howard, J.A.E., Agenbag, J., Jarre, A., 2012. Regime-shifts in the southern Benguela shelf and inshore region. Prog. Oceanogr. 106:80–95. http://dx.doi.org/10.1016/j.pocean.2012.07.001.

Blamey, L.K., Shannon, L.J., Bolton, J.J., Crawford, R.J.M., Dufois, F., Evers-King, H., Griffiths, C.L., Hutchings, L., Jarre, A., Rouault, M., Watermeyer, K.E., Winker, H., 2015. Ecosystem changes in the southern Benguela and the underlying processes. J. Mar. Syst. 144:9–29. http://dx.doi.org/10.1016/j.jmarsys.2014.11.006.

Bograd, S.J., Schroeder, I., Sarkar, N., Qiu, X., Sydeman, W.J., Schwing, F.B., 2009. Phenology of coastal upwelling in the California Current. Geophys. Res. Lett. 36, L01602. http://dx.doi.org/10.1029/2008GL035933.

Capet, X.J., Marchesiello, P., Williams, J.C., 2004. Upwelling response to coastal wind profiles. Geophys. Res. Lett. 31, L13311. http://dx.doi.org/10.1029/2004GLO20123.

Cardone, V.J., Greenwood, J.G., Cane, M.A., 1990. On trends in historical marine wind data. J. Clim. 3:113–127. http://dx.doi.org/10.1175/1520-0442(1990)003<0113:OTIHMW>2.0.CO;2.

Chaigneau, A., Eldin, G., Dewitte, B., 2009. Eddy activity in the four major upwelling systems from satellite altimetry (1992-2007). Prog. Oceanogr. 83:117–123. http://dx.doi.org/10.1016/j.pocean.2009.07.012.

Chavez, F.P., Messié, M., 2009. A comparison of eastern boundary upwelling ecosystems. Prog. Oceanogr. 83:80–96. http://dx.doi.org/10.1016/j.pocean.2009.07.032.

Chelton, D.B., Schlax, M.G., Freilich, M.H., Milliff, R.F., 2004. Satellite measurements reveal persistent small-scale features in ocean winds. Science 303:978–983. http://dx.doi.org/10.1126/science.1091901.

Chen, Z., Yan, X.-H., Jo, Y.-H., Jiang, L., Jiang, Y., 2012. A study of Benguela upwelling system using different upwelling indices derived from remotely sensed data. Cont. Shelf Res. 45:27–33. http://dx.doi.org/10.1016/j.csr.2012.05.013.

Coetzee, J.C., van der Lingen, C.D., Hutchings, L., Fairweather, T., 2008. Has the fishery contributed to a major shift in the distribution of South African sardine? ICES J. Mar. Sci. 65:1676–1688. http://dx.doi.org/10.1093/icesjms/fsn184.

Colas, F., Capet, X., McWilliams, J.C., Shchepetkin, A., 2008. 1997-1998 El Niño off Peru: a numerical study. Prog. Oceanogr. 79:138–155. http://dx.doi.org/10.1016/j.pocean.2008.10.015.

Crawford, R.J.M., Makhado, A.B., Whittington, P.A., Randall, R.M., Oosthuizen, W.H., Waller, L.J., 2015. A changing distribution of seabirds in South Africa – the possible impact of climate and its consequences. Front. Ecol. Evol. 3 (10):1–10. http://dx.doi.org/10.3389/fevo.2015.00010.

Emery, W.J., Thomson, R.E., 2001. Data Analysis Methods in Physical Oceanography. (683 pp.). Elsevier, Amsterdam.

García-Reyes, M., Sydeman, W.J., Black, B.A., Rykaczewski, R.R., Schoeman, D.S., Thompson, S.A., Bograd, S.J., 2013. Relative influence of oceanic and terrestrial pressure systems in driving upwelling-favorable winds. Geophys. Res. Lett. 40 (19): 5311–5315. http://dx.doi.org/10.1002/2013GL057729.

García-Reyes, M., Largier, J.L., Sydeman, W.J., 2014. Synoptic-scale upwelling indices and predictions of phyto- and zooplankton populations. Prog. Oceanogr. 120:177–188. http://dx.doi.org/10.1016/j.pocean.2013.08.004.

García-Reyes, M., Lamont, T., Sydeman, W.J., Black, B.A., Rykaczewski, R.R., Thompson, S.A., Bograd, S.J., 2017. A Comparison of Modes of Upwelling Variability in the Benguela and California Current Ecosystems submitted to this issue.

Goschen, W.S., Schumann, E.H., Bernard, K.S., Bailey, S.E., Deyzel, S.H.P., 2012. Upwelling and ocean structures off Algoa Bay and the south-east coast of South Africa. Afr. J. Mar. Sci. 34:525–536. http://dx.doi.org/10.2989/1814232X.2012.749810.

Gruber, N., Lachkar, Z., Frenzel, H., Marchesiello, P., Münnich, M., McWilliams, J.C., Nagai, T., Plattner, G.-K., 2011. Eddy-induced reduction of biological production in eastern boundary upwelling systems. Nat. Geosci. 4:787–792. http://dx.doi.org/10.1038/NGEO1273.

Hutchings, L., van der Lingen, C.D., Shannon, L.J., Crawford, R.J.M., Verheye, H.M.S., Bartholomae, C.H., van der Plas, A.K., Louw, D., Kreiner, A., Ostrowski, M., Fidel, Q., Barlow, R.G., Lamont, T., Coetzee, J., Shillington, F., Veitch, J., Currie, J.C., Monteiro, P.M.S., 2009. The Benguela Current: an ecosystem in four components. Prog. Oceanogr. 83:15–32. http://dx.doi.org/10.1016/j.pocean.2009.07.046.

Iles, A.C., Guohier, T.C., Menge, B.A., Stewart, J.S., Haupt, A.J., Lynch, M.C., 2012. Climate-driven trends and ecological implications of event-scale upwelling in the California Current System. Glob. Chang. Biol. 18:783–796. http://dx.doi.org/10.1111/j.1365-2486.2011.02567.x.

IPCC, 2014. Climate change 2014: synthesis report. In: Core Writing Team, Pachauri, R.K., Meyer, L.A. (Eds.), Contribution of Working Groups I, II and III to the Fifth Assessment Report of the Intergovernmental Panel on Climate Change. IPCC, Geneva, Switzerland (151 pp).

Jarre, A., Hutchings, L., Kirkman, S.P., Kreiner, A., Tchipalanga, P.C.M., Kainge, P., Uanivi, U., van der Plas, A.K., Blamey, L.K., Coetzee, J.C., Lamont, T., Samaai, T., Verheye, H.M., Yemane, D.G., Axelsen, B.E., Ostrowski, M., Stenevik, E.K., Loeng, H., 2015. Synthesis: climate effects on biodiversity, abundance and distribution of marine organisms in the Benguela. Fish. Oceanogr. 24:122–149. http://dx.doi.org/10.1111/fog.12086 (Supplement 1).

Kanamitsu, M., Ebisuzaki, W., Woollen, J., Yang, S.-K., Hnilo, J.J., Fiorino, M., Potter, G.L., 2002. NCEP-DOE AMIP-II Reanalysis (R-2). Bull. Am. Meteorol. Soc. 83:1631–1643. http://dx.doi.org/10.1175/BAMS-83-11-1631.

Kent, E.C., Fangohr, S., Berry, D.I., 2013. A comparative assessment of monthly mean wind speed products over the global ocean. Int. J. Climatol. 33:2520–2541. http://dx.doi.org/10.1002/joc.3606.

Large, W.G., Pond, S., 1981. Open ocean momentum flux measurements in moderate to strong winds. J. Phys. Oceanogr. 11, 324–336.

Lett, C., Veitch, J., van der Lingen, C., Hutchings, L., 2007. Assessment of an environmental barrier to transport of ichthyoplankton from the southern to the northern Benguela ecosystem. Mar. Ecol. Prog. Ser. 347:247–259. http://dx.doi.org/10.3354/meps06982.

van der Lingen, C.D., Hutchings, L., Lamont, T., Pitcher, G.C., 2016. Climate change, dinoflagellate blooms and sardine in the southern Benguela Current Large Marine Ecosystem. Environ. Dev. 17:230–243. http://dx.doi.org/10.1016/j.envdev.2015.09.004.

MacCall, A.D., Sydeman, W.J., Davison, P.C., Thayer, J.A., 2016. Recent collapse of northern anchovy biomass off California. Fish. Res. 175:87–94. http://dx.doi.org/10.1016/j.fishres.2015.11.013.

Marchesiello, P., Estrade, P., 2010. Upwelling limitation by onshore geostrophic flow. J. Mar. Res. 68:37–62. http://dx.doi.org/10.1357/002224010793079004.

Marchesiello, P., Lefèvre, J., Vega, A., Couvelard, X., Menkes, C., 2010. Coastal upwelling, circulation and heat balance around New Caledonia's barrier reef. Mar. Pollut. Bull. 61:432–448. http://dx.doi.org/10.1016/j.marpolbul.2010.06.043.

Messié, M., Ledesma, J., Kolber, D.D., Michisaki, R.P., Foley, D.G., Chavez, F.P., 2009. Potential new production estimates in four eastern boundary upwelling ecosystems. Prog. Oceanogr. 83:151–158. http://dx.doi.org/10.1016/j.pocean.2009.07.018.

Narayan, N., Paul, A., Mulitza, S., Schulz, M., 2010. Trends in coastal upwelling intensity during the late 20th century. Ocean Sci. 6:815–823. http://dx.doi.org/10.5194/os-6-815-2010.

Oerder, V., Colas, F., Echevin, V., Codron, F., Tam, J., Belmadani, A., 2015. Peru-Chile upwelling dynamics under climate change. J. Geophys. Res. Oceans Atmos. 120:1152–1172. http://dx.doi.org/10.1002/2014JC010299.

Pauly, D., Christensen, V., 1995. Primary production required to sustain global fisheries. Nature 374, 255–257.

Risien, C.M., Chelton, D.B., 2008. A global climatology of surface wind and wind tress fields from eight years of QuikSCAT scatterometer data. J. Phys. Oceanogr. 38:2379–2413. http://dx.doi.org/10.1175/2008JPO3881.1.

Rossi, V., López, C., Sudre, J., Hernández-García, E., Garçon, V., 2008. Comparative study of mixing and biological activity of the Benguela and Canary upwelling systems. Geophys. Res. Lett. 35, L11602. http://dx.doi.org/10.1029/2008GL033610.

Rouault, M., Pohl, B., Penven, P., 2010. Coastal oceanic climate change and variability from 1982 to 2009 around South Africa. Afr. J. Mar. Sci. 32:237–246. http://dx.doi.org/10.2989/1814232X.2010.501563.

Roy, C., Weeks, S., Rouault, M., Nelson, G., Barlow, R., van der Lingen, C., 2001. Extreme oceanographic events recorded in the southern Benguela during the 1999-2000 summer season. S. Afr. J. Sci. 97, 465–471.

Roy, C., van der Lingen, C.D., Coetzee, J.C., Lutjeharms, J.R.E., 2007. Abrupt environmental shift associated with changes in distribution of Cape anchovy *Engraulis encrasicolus* spawners in the southern Benguela. Afr. J. Mar. Sci. 29:309–319. http://dx.doi.org/10.2989/AJMS.2007.29.3.1.331.

Roy, C., Herbette, S., van der Lingen, C., Hermes, J., 2016. Strengths and weaknesses of climate re-analyses to quantify wind variability: a focus on the 20th Century Reanalysis in the Benguela and adjacent areas. Benguela Symposium 2016: Opportunity, Challenge and Change, 15–18 November, Cape Town, South Africa.

Rykaczewski, R.R., Checkley Jr., D.M., 2008. Influence of ocean winds on the pelagic ecosystem in upwelling regions. Proc. Natl. Acad. Sci. U. S. A. 105:1965–1970. http://dx.doi.org/10.1073/pnas.0711777105.

Rykaczewski, R.R., Dunne, J.P., Sydeman, W.J., García-Reyes, M., Black, B.A., Bograd, S.J., 2015. Poleward displacement of coastal upwelling-favourable winds in the ocean's eastern boundary currents through the 21st century. Geophys. Res. Lett. 42: 6424–6431. http://dx.doi.org/10.1002/2015GL064694.

Schroeder, I.D., Black, B.A., Sydeman, W.J., Bograd, S.J., Hazen, E.L., Santora, J.A., Wells, B.K., 2013. The North Pacific High and wintertime pre-conditioning of California current productivity. Geophys. Res. Lett. 40:541–546. http://dx.doi.org/10.1002/grl.50100.

Schumann, E.H., 1998. The coastal ocean off southeast Africa, including Madagascar. The Sea 11, 557–582.

Schumann, E.H., 1999. Wind-driven mixed layer and coastal upwelling processes off the south coast of South Africa. J. Mar. Res. 57:671–691. http://dx.doi.org/10.1357/002224099321549639.

Schumann, E.H., Ross, G.J.B., Goschen, W.S., 1988. Cold water events in Algoa Bay and along the Cape south coast, South Africa, in March/April 1987. S. Afr. J. Sci. 84, 579–584.

Schumann, E.H., Martin, J.A., 1991. Climatological aspects of the coastal wind field at Cape Town, Port Elizabeth and Durban. S. Afr. Geogr. J. 73, 48–51.

Schumann, E.H., Perrins, L.-A., Hunter, I.T., 1982. Upwelling along the South Coast of the Cape Province, South Africa. S. Afr. J. Sci. 78, 238–242.

Schumann, E.H., Cohen, A., Jury, M.R., 1995. Coastal sea surface temperature variability along the south coast of South Africa and the relationship to regional and global climate. J. Mar. Res. 53:231–248. http://dx.doi.org/10.1357/0022240953213205.

Schwing, F.B., Bond, N.A., Bograd, S.J., Mitchell, T., Alexander, M.A., Mantua, N., 2006. Delayed coastal upwelling along the U.S. West Coast in 2005: a historical perspective. Geophys. Res. Lett. 33:L22S01. http://dx.doi.org/10.1029/2006GL026911.

Shillington, F.A., Reason, C.J.C., Duncombe Rae, C.M., Florenchie, P., Penven, P., 2006. Large Scale Physical Variability of the Benguela Current Large Marine Ecosystem (BCLME). In: Shannon, V., et al. (Eds.), Benguela: Predicting a Large Marine Ecosystem, Large Mar. Ecosyst. Vol. 14. Elsevier, Amsterdam, Netherlands, pp. 49–70.

Sydeman, W.J., Garćia-Reyes, M., Schoeman, D.S., Rykaczewski, R.R., Thompson, S.A., Black, B.A., Bograd, S.J., 2014. Climate change and wind intensification in coastal upwelling ecosystems. Science 345:77–80. http://dx.doi.org/10.1126/science.1251635.

Tim, N., Zorita, E., Hünicke, B., 2015. Decadal variability and trends of the Benguela upwelling system simulated in a high-resolution ocean simulation. Ocean Sci. 11: 483–502. http://dx.doi.org/10.5194/os-11-483-2015.

Trenberth, K.E., Large, W.G., Olson, J.G., 1990. The mean annual cycle in global ocean wind stress. J. Phys. Oceanogr. 20:1742–1760. http://dx.doi.org/10.1175/1520-0485(1990)020<1742:TMACIG>2.0.CO;2.

Veitch, J., Penven, P., Shillington, F., 2010. Modeling equilibrium dynamics of the Benguela current system. J. Phys. Oceanogr. 40:1942–1964. http://dx.doi.org/10.1175/2010JPO4382.1.

Walker, N.D., 1986. Satellite observations of the Agulhas Current and episodic upwelling south of Africa. Deep-Sea Res. Part A 33:1083–1106. http://dx.doi.org/10.1016/0198-0149(86)90032-4.
Wang, D., Gouhier, T.C., Menge, B.A., Ganguly, A.R., 2015. Intensification and spatial homogenization of coastal upwelling under climate change. Nature 518:390–394. http://dx.doi.org/10.1038/nature14235.
Watermeyer, K.E., Hutchings, L., Jarre, A., Shannon, L.J., 2016. Patterns of distribution and spatial indicators of ecosystem change based on key species in the Southern Benguela. PLoS One 11 (7), e0158734. http://dx.doi.org/10.1371/journal.pone.0158734.
Zwolinski, J.P., Demer, D.A., 2012. A cold oceanographic regime with high exploitation rates in the Northeast Pacific forecasts a collapse of the sardine stock. Proc. Natl. Acad. Sci. 109:4175–4180. http://dx.doi.org/10.1073/pnas.1113806109.